J Anal (2019) 27:103–120
https://doi.org/10.1007/s41478-018-0108-3

ORIGINAL RESEARCH PAPER

Unsteady MHD reactive flow of second grade fluid through porous medium in a rotating parallel plate channel

M. VeeraKrishna[1] · G. Subba Reddy[1]

Received: 28 January 2018 / Accepted: 7 June 2018 / Published online: 13 June 2018

Abstract We considered the transient MHD flow of a reactive second grade fluid through a porous medium between two infinitely long horizontal parallel plates where one of the plate is uniform accelerated motion in the presence of a uniform transverse magnetic field with Arrhenius reaction rate. The transient momentum equations are solved analytically using the Laplace transform technique. The velocity and temperature is presented in graphical form and discussed computationally. The shear stress and Nusselt number are also obtained analytically and computationally discussed. Our results divulge that the effects of magnetic field, rotation, exothermic reaction and variable thermal conductivity have significant impact on the hydromagnetic flow and heat transfer.

Keywords Heat and mass transfer · MHD flows · Parallel plate · Porous medium · Reactive flow · Second grade fluids

Mathematics Subject Classification 76A05 · 76E06 · 76N20 · 76V05 · 76W05

List of symbols

(u, w)	The fluid velocity components
(x, z)	Co-ordinate system
q	The fluid density
ν	The kinematics viscosity
σ	The electrical conductivity and

✉ M. VeeraKrishna
veerakrishna_maths@yahoo.com

G. Subba Reddy
gsreddy.lucky@gmail.com

[1] Department of Mathematics, Rayalaseema University, Kurnool, Andhra Pradesh, India

p	The fluid pressure
k	The thermal conductivity
C_{p}	The specific heat at constant pressure
T	The temperature of the fluid
Q	The heat of reaction
C_0	The initial concentration of reacting species
A	The rate constant
R	The universal gas constant
M^2	The magnetic field parameter (Hartmann number)
D	The Darcy parameter (permeability parameter)
K^2	The rotation parameter
S	The second grade fluid parameter
Ec	The Eckert number
λ	The Frank-Kamenetskii parameter or reaction rate parameter
ε	The activation energy parameter
δ	Thermal conductivity variation parameter and
Pr	The Prandtl number

1 Introduction

Studies on heat transfer in MHD flow of non-Newtonian fluids find its relevance in several geological, petrochemical, and industrial applications. The MHD flow is a very important phenomenon that is widely encountered in this era of industrialization. It has numerous applications, for example in lubrication of mechanical devices where a thin film of lubricant is attached to the surface slipping over one another or when the surfaces are coated with special coatings to minimize the friction between them. From applications' point of view, studies on transport reactive fluids in porous media are very important since they occur in many important areas like water treatment using fixed beds, agriculture, oil recovery, ground water flows, geothermal engineering, and exhaust systems in combustion, material processing, and reservoir engineering.

In fluid dynamics, Couette flow refers to the laminar flow of a viscous incompressible fluid in the space between two parallel plates, one of which is moving and the other remains fixed. Couette flow occurs in fluid machinery involving moving parts and is especially important for hydrodynamic lubrication.

Couette flow has been used as the fundamental method for the measurement of viscosity and as a means of estimating the drag force in many wall driven applications. The MHD is concerned with the mutual interaction of conducting fluid flow and magnetic field. The fluids being investigated must be electrically conducting, which limits the fluids to liquid metals, hot ionized gases (plasmas) and strong electrolytes. The study of magnetic field effects has considerable interest in the technical fields due to its applications in industrial technology. These applications include MHD power generators, cooling of nuclear reactors, liquid metal flow control, micro MHD pumps, high-temperature plasmas, biological transportation, drying processes and solidification of binary alloy.

Many researchers like AnwarBég et al. [1], Chandran et al. [2], Chauhan and Agrawal [3] examined the effect of rotation on an unsteady hydromagnetic Couette flow. Chinyoka and Makinde [4] discussed the analysis of transient generalized Couette flow of a reactive variable viscosity third grade liquid with asymmetric convective cooling. Cramer and Pai [5], Das et al. [6–8] and Gosh et al. [9] investigated an unsteady MHD Couette flows in a rotating system. Ghosh et al. [10] studied effects of Hall currents on an unsteady MHD Couette flow. Jana et al. [11] and Jana and Datta [12] discussed MHD flows through porous medium. The combined effects of Hall and ion-slip currents on an unsteady MHD Couette flows in a rotating system were examined by Jha and Apere [13]. Jha and Apere [14] presented an MHD Couette flow in a rotating system with suction injection. Jha and Apere [15] studied Hall effects on the MHD flow in rotating porous media. Jha et al. [16] discussed the unsteady MHD free convective Couette flow between vertical porous plates with thermal radiation. Jha et al. [17] discussed an exact solution on fully developed MHD natural convection flow in a vertical annular microchannel. The second law analysis of Couette flow of a reactive fluid with variable viscosity under Arrhenius kinetics was carried out by Kobo and Makinde [18]. Makinde [19] presented a steady flow of a reactive variable viscosity fluid. Makinde and Onyejekwe [20], Makinde [21] and Makinde and Franks [22] studied MHD generalized Couette flows and heat transfer with variable viscosity. Muzychka and Yovanovich [23] studied the unsteady viscous flows and Stokes' first problem. Nanda and Mohanty [24] investigated hydromagnetic flows in a rotating channel. More recently, Nayak and Dash [25] have studied the MHD flow through a porous medium in a rotating channel. Ramzan and Bilal [26] found the series solution of time dependent MHD second grade incompressible nanofluid towards a stretching sheet. Recently, Ramzan et al. [27] studied three dimensional second grade nanofluid flow with effects of thermal radiation and mixed convection over an exponential stretched surface under the influence of convective boundary conditions. Ramzan et al. [28] examined the mixed convective flow of Maxwell nanofluid with Soret and Dufour effects through a porous medium. Ramzan et al. [29] discussed the thermal-diffusion (Dufour) and diffusion-thermo (Soret) effects on the mixed convection boundary layer flow of viscoelastic nanofluid flow over a vertical stretching surface in a porous medium. A mathematical model has been established to study the MHD second grade nanofluid flow past a bidirectional stretched surface by Ramzan et al. [30]. Numerical simulation of steady two dimensional flow of Casson nanofluid with the effects of MHD, chemical reaction and thermal radiation in the presence of non-uniform heat source/sink through a permeable medium is investigated by Ramzan et al. [31]. Ramzan et al. [32] investigated the flow of micropolar nanofluid due to a rotating disk in the presence of magnetic field and partial slip condition. Seth et al. [33], Seth and Maiti [34], Seth and Ghosh [35] presented the MHD Couette flow and heat transfer in a rotating system. Seth et al. [36] investigated the unsteady hydromagnetic Couette flow induced due to accelerated movement of one of the porous plates of the channel in a rotating system. Singh and Pathak [37] studied Hall effects on the MHD flow in rotating porous media. Seth and Singh [38] discussed effects of Hall current on unsteady MHD Couette flow of class-II in a rotating system. Recently,

Seth et al. [39] have studied an unsteady MHD convection flow of a heat absorbing fluid within a rotating vertical channel. Seth and Singh [40] have described the mixed convection flow in a rotating channel. Singh et al. [41] studied the MHD Couette flow with rotation. Swarnalathamma and Veera Krishna [42] discussed the peristaltic hemodynamic flow of couple stress fluid through a porous medium under the influence of magnetic field with slip effect. Theuri and Makinde [43] discussed thermodynamic analysis of variable viscosity MHD unsteady generalized Couette flow with permeable walls. Veera Krishna and Gangadhar Reddy [44] and Veera Krishna and Subba Reddy [45] discussed MHD free convective rotating flows. Veera Krishna and Swarnalathamma [46] discussed convective heat and mass transfer on MHD peristaltic flow of Williamson fluid with the effect of inclined magnetic field. Veera Krishna et al. [47] discussed heat and mass transfer on unsteady MHD oscillatory flow of blood through porous arteriole. The effects of radiation and Hall current on an unsteady MHD free convective flow in a vertical channel filled with a porous medium have been studied by Veera Krishna et al. [48]. The heat generation/absorption and thermo-diffusion on an unsteady free convective MHD flow of radiating and chemically reactive second grade fluid near an infinite vertical plate through a porous medium and taking the Hall current into account have been studied by Veera Krishna and Chamkha [49].

Almost all the above mentioned studies have assumed that fluid properties are constant. However experiments indicate that this can only hold, if temperature does not change rapidly or impulsively in any particular way. Hence more accurate prediction of flow and heat transfer can only be obtained by considering variations of fluid and electromagnetic properties, especially variations of fluid viscosity, thermal conductivity as well as electrical conductivity with temperature. The study of reactive viscous fluids under a Couette flow scenario in a rotating system is extremely important in understanding lubricant hydrodynamics and heat transfer in engineering and industrial systems. Generally speaking, most lubricants used in both engineering and industrial processes are reactive e.g. hydrocarbon oils, polyglycols,

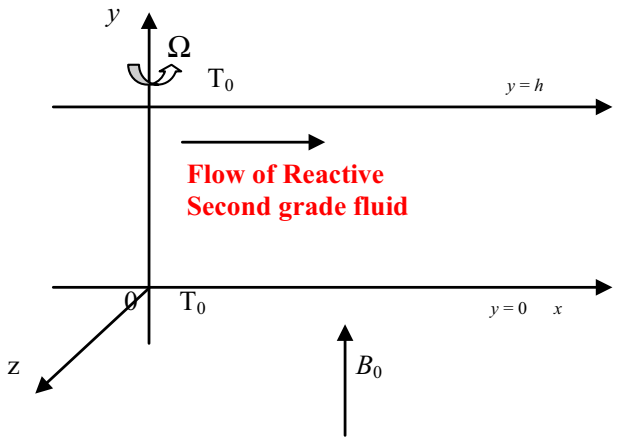

Fig. 1 Physical configuration of the problem

synthetic esters, and polyphenylethers and their efficiency depends largely on the temperature variation from time to time. It is thus important to determine the heat transfer conditions and thermal loading properties of viscous reactive fluids to gauge their effectiveness as lubricants.

Motivated by the above studies, in this paper we have to examine the effects of rotation and the magnetic field on the transient MHD flow of a reactive second grade fluid between infinite horizontal parallel plates in a rotating system.

2 Formulation and solution of the problem

We consider the unsteady MHD couttee flow of second grade fluid between two infinite horizontal parallel plates of distance h when the fluid and the plates rotate in unison with uniform angular velocity Ω about an axis normal to the plates. The y-axis is taken normal to the x-axis and the z-axis is taken normal to the xz-plane (see Fig. 1), lying in the plane of the lower plate. Initially, at time $t \leq 0$, the two plates and the fluid are assumed to be at the same temperature T_0 and stationary. At time $t > 0$, the plate at $y = h$ starts to move in its own plane with the velocity $U(t)$ and its temperature is T_0 whereas the plate at $y = 0$ is stationary and maintained at a constant temperature T_0. Since the plates are infinitely long along the x- and y-directions, all physical quantities will be functions of y and t only.

It is assumed that induced magnetic field produced by the fluid motion is negligible in comparison with the applied one so that we take magnetic field as $B = (0, 0, B_0)$. We assume $E = (0, 0, 0)$. Under the above assumptions, the Navier–Stokes equations of motion in a rotating frame of reference

$$\frac{\partial u}{\partial t} + 2\Omega w = -\frac{1}{\rho}\frac{\partial p}{\partial x} + \nu\frac{\partial^2 u}{\partial y^2} + \frac{\alpha}{\rho}\frac{\partial^3 u}{\partial y^2 \partial t} - \frac{\sigma B_0^2}{\rho}u - \frac{\nu}{k}u \tag{1}$$

$$0 = -\frac{1}{\rho}\frac{\partial p}{\partial y} \tag{2}$$

$$\frac{\partial w}{\partial t} - 2\Omega u = -\frac{1}{\rho}\frac{\partial p}{\partial z} + \nu\frac{\partial^2 w}{\partial y^2} + \frac{\alpha}{\rho}\frac{\partial^3 w}{\partial y^2 \partial t} - \frac{\sigma B_0^2}{\rho}w - \frac{\nu}{k}w \tag{3}$$

The initial and boundary conditions are

$$u = w = 0, \quad t \leq 0, \text{ for } 0 \leq y \leq h \tag{4a}$$

$$u = w = 0, \quad t > 0, \text{ for } y = 0 \tag{4b}$$

$$u = w = U(t), \quad t > 0, \text{ for } y = h \tag{4c}$$

Equations (1) and (3) can be written as using the boundary condition at $y = h$ and we have

$$\frac{\partial U}{\partial t} = -\frac{1}{\rho}\frac{\partial p}{\partial x} - \frac{\sigma B_0^2}{\rho}U - \frac{\nu}{k}w \ , \quad -2\Omega u = -\frac{1}{\rho}\frac{\partial p}{\partial z} \tag{5}$$

On the use of (5), the momentum Eqs. (1) and (2) along x and z-directions become

$$\frac{\partial w}{\partial t} - 2\Omega(u - U) = \nu\frac{\partial^2 w}{\partial y^2} + \frac{\alpha}{\rho}\frac{\partial^3 w}{\partial y^2 \partial t} - \frac{\sigma B_0^2}{\rho}w - \frac{\nu}{k}w \tag{6}$$

$$\frac{\partial u}{\partial t} + 2\Omega w = \frac{\partial U}{\partial t} + \nu\frac{\partial^2 u}{\partial y^2} + \frac{\alpha}{\rho}\frac{\partial^3 u}{\partial y^2 \partial t} - \frac{\sigma B_0^2}{\rho}(u - U) - \frac{\nu}{k}(u \ - U) \tag{7}$$

Introducing non-dimensional variables

$$y * = \frac{y}{h}, \ u^* = \frac{u}{u_0}, \ w^* = \frac{w}{w_0}, \ t^* = \frac{\nu t}{h^2}, \ U = u_0 f(t) \tag{8}$$

Making use of non-dimensional variables, Eqs. (6) and (7) become (dropping asterisks)

$$\frac{\partial u}{\partial t} + 2K^2 w = \frac{\partial f}{\partial t} + \frac{\partial^2 u}{\partial y^2} + S\frac{\partial^3 u}{\partial y^2 \partial t} - \left(M^2 + \frac{1}{D}\right)(u - f) \tag{9}$$

$$\frac{\partial w}{\partial t} - 2K^2(u - f) = \frac{\partial^2 w}{\partial y^2} + S\frac{\partial^3 w}{\partial y^2 \partial t} - \left(M^2 + \frac{1}{D}\right)w \tag{10}$$

where, $M^2 = \frac{\sigma B_0^2 h^2}{\rho \nu}$ is the magnetic field parameter (Hartmann number), $D = \frac{k}{h^2}$ is the Darcy parameter (permeability parameter), $K^2 = \frac{\Omega h^2}{\nu}$ is the rotation parameter and $S = \frac{\alpha}{\rho h^2}$ is the second grade fluid parameter.

The corresponding initial and boundary conditions (4) become

$$u = w = 0, \quad t \leq 0, \ \text{for} \ 0 \leq y \leq 1 \tag{11a}$$

$$u = w = 0, \quad t > 0, \ \text{for} \ y = 0 \tag{11b}$$

$$u = w = f(t), \quad t > 0, \ \text{for} \ y = 1 \tag{11c}$$

Combining Eqs. (9) and (10), we get

$$\frac{\partial q}{\partial t} - 2iK^2 q = \frac{\partial^2 q}{\partial y^2} + S\frac{\partial^3 q}{\partial y^2 \partial t} - \left(M^2 + \frac{1}{D}\right)q \tag{12}$$

where $q = u + iw - f$ and $i = \sqrt{-1}$

The initial and boundary conditions for $q = (y,\ t)$ are

$$q = 0, \quad t \le 0, \ \text{for} \ 0 \le y \le 1 \tag{13a}$$

$$q = -f, \quad t > 0, \ \text{for} \ y = 0 \tag{13b}$$

$$q = 0, \quad t > 0, \ \text{for} \ y = 1 \tag{13c}$$

Taking the Laplace transform of Eq. (12) and on the use of (13a, 13b, 13c), we have

$$(1 + sS)\frac{\partial^2 \bar{q}}{\partial y^2} - \left(s + M^2 - 2iK^2 + \frac{1}{D}\right)\bar{q} = 0 \tag{14}$$

The boundary conditions for $\bar{q}(y, s)$ are

$$\bar{q}(0, s) = -\bar{f}(s) \ \text{ and } \ \bar{q}(1, s) = 0 \tag{15}$$

where, $\bar{f}(s)$ is the Laplace transform of $f(t)$

Solutions of Eq. (14) subject to the boundary conditions (15) are given by

$$\bar{q}(y, s) = -\bar{f}(s)\frac{\sinh\ g(s)(1 - y)}{\sinh\ g(s)} \tag{16}$$

where, $g(s) = \sqrt{\frac{s + M^2 - 2iK^2 + \frac{1}{D}}{1 + sS}}$

The upper plate has been set into motion with a speed $f(t) = t$, which corresponds to the accelerated motion. Then the inverse Laplace transforms of Eq. (16) gives the solution for the velocity components as

$$\begin{aligned} q = t - t\,&\frac{\sinh(a - ib)(1 - y)}{\sinh(a - ib)} + \frac{1}{2(a - ib)\sinh^2(a - ib)} \\ &\left[\cosh(a - ib)\ \sinh(a - ib)(1 - y) - (1 - y)\sinh(a - ib)\ \cosh(a - ib)y\right] \\ &+ 2\ \sum_{n=1}^{\infty} (-1)^n\, n\pi\, e^{-\left((\alpha - i\beta) + n^2\pi^2\right)\, t} \sin n\pi y \end{aligned} \tag{17}$$

$$a,\, b = \frac{1}{\sqrt{2}}\left[\left\{\left(\frac{\left(M^2+(1/D)\right)+2SK^2}{1+S^2}\right)^2+\left(\frac{2K^2+S\left(M^2+(1/D)\right)}{1+S^2}\right)^2\right\}^{\frac{1}{2}}\right.$$

where,

$$\left.\pm\frac{\left(M^2+(1/D)\right)+2SK^2}{1+S^2}\right]^{\frac{1}{2}}$$

In the inertial frame of reference ($K^2 = 0$, $D^{-1} = 0, S = 0$), the present problem reduces to the problem studied by Makinde and Franks [22]. Also reduces to Das et al. [34] when $D^{-1} = 0, S = 0$.

The shear stresses at the plates $y = 0$ and $y = 1$ are by

$$\tau_L = \left(\frac{dq}{dy}\right)_{y=0} = t\,(a-ib)\coth(a-ib) + \frac{1}{2(a-ib)\sinh^2(a-ib)}$$
$$[\cosh(a-ib)\ \sinh(a-ib) - (a-ib)] + 2\sum_{n=0}^{\infty}(-1)^n n^2\pi^2\, e^{-\left((\alpha-i\beta)+n^2\pi^2\right)t} \tag{18}$$

$$\tau_U = \left(\frac{dq}{dy}\right)_{y=1} = t\,(a-ib)\mathrm{csch}(a-ib) + \frac{1}{2(a-ib)\sinh^2(a-ib)}$$
$$[\sinh(a-ib) - (a-ib)\cosh(a-ib)] + 2\sum_{n=0}^{\infty} n^2\pi^2\, e^{-\left((\alpha-i\beta)+n^2\pi^2\right)t} \tag{19}$$

The energy equation taking viscous and Joule dissipations into account is given by

$$\rho\, C_p\frac{\partial T}{\partial t} = \frac{\partial}{\partial t}\left(k_1\frac{\partial T}{\partial y}\right) + \mu\left[\left(\frac{\partial u}{\partial y}\right)^2+\left(\frac{\partial w}{\partial y}\right)^2\right]$$
$$+\left(\sigma B_0^2+\frac{\nu}{k}\right)\left[(u-U)^2+w^2\right] + Q\, C_0 A e^{-\frac{E}{Rt}} \tag{20}$$

The first term on right hand side is for heat conduction, the second term for viscous dissipation, the third term for Joule heating and the fourth term for Arrhenius reaction.

The initial and boundary conditions for the temperature are

$$T = T_0, \quad t \le 0, \ \text{for}\ 0 \le y \le h \tag{21a}$$

$$T = T_0, \quad t > 0, \ \text{for}\ y = 0 \tag{21b}$$

$$T = T_0, \quad t > 0, \ \text{for}\ y = h \tag{21c}$$

Following from Makinde and Franks [22], the fluid thermal conductivity is assumed to vary exponentially with temperature such that

$$K(T) = K_0\, e^{m(T-T_0)} \approx K_0(1 + m\,(T - T_0)) \tag{22}$$

where, the parameter m may be positive for some fluids such as air or water vapour or negative for others like benzene. Introducing the non-dimensional variable, Eq. (20) becomes

$$\begin{aligned} \Pr \frac{\partial \theta}{\partial t} = \frac{\partial}{\partial y}\left((1 + \delta\theta\frac{\partial \theta}{\partial y}\right) + \lambda\, e^{\frac{\theta}{1+\varepsilon\theta}} \\ + \Pr\, Ec\left[\left(\frac{\partial u}{\partial y}\right)^2 + \left(\frac{\partial w}{\partial y}\right)^2 + \left(M^2 + \frac{1}{D}\right)\left((u-1)^2 + w^2\right)\right] \end{aligned} \tag{23}$$

where, $Ec = \frac{Eu_0^2}{C_p R T_0^2}$ is the Eckert number which expresses the relationship between a flow's kinetic energy and enthalpy, $\lambda = \frac{QC_0Ah^2}{Ek_0T_0^2}\, e^{-\frac{E}{RT_0}}$ the Frank-Kamenetskii parameter or reaction rate parameter, $\varepsilon = \frac{RT_0}{E}$ the activation energy parameter, $\delta = \frac{mRT_0^2}{E}$ thermal conductivity variation parameter and $\Pr = \frac{\rho\nu C_p}{k_0}$ the Prandtl number which is defined as the ratio of momentum diffusivity (kinematic viscosity) to thermal diffusivity.

The corresponding initial and boundary conditions are

$$\theta(y,\, 0) = 0, \quad \text{for } 0 \le y \le 1 \tag{24a}$$

$$\theta(0,\, t) = 0,\ \theta(1,\, t) = 0 \text{ for } t > 0 \tag{24b}$$

The local Nusselt number (surface heat transfer gradient) at the lower plate and upper plate are given by

$$Nu_L = -\left(\frac{\partial \theta}{\partial y}\right)_{y=0} \tag{25}$$

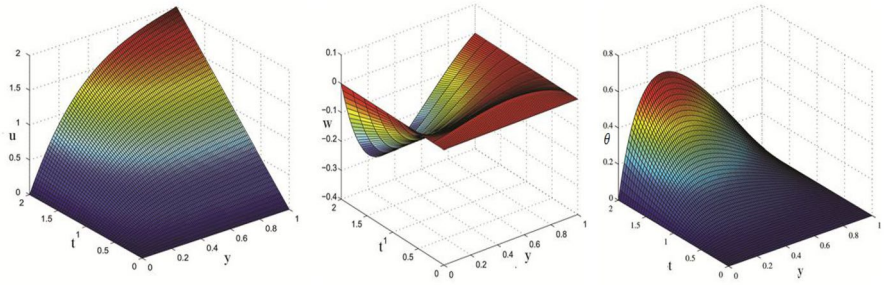

Fig. 2 The velocity profiles for u and w, temperature profile for θ with time

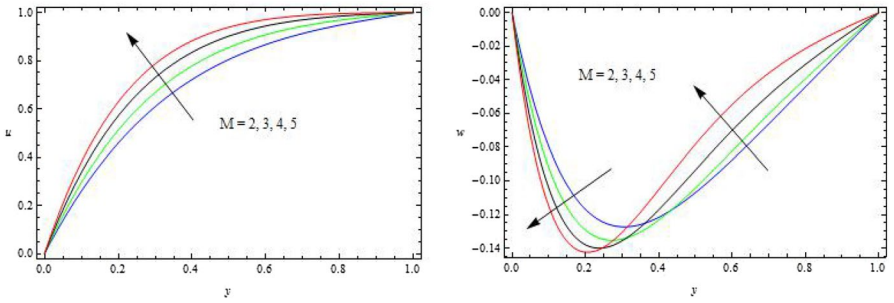

Fig. 3 The velocity profiles for u and w against M

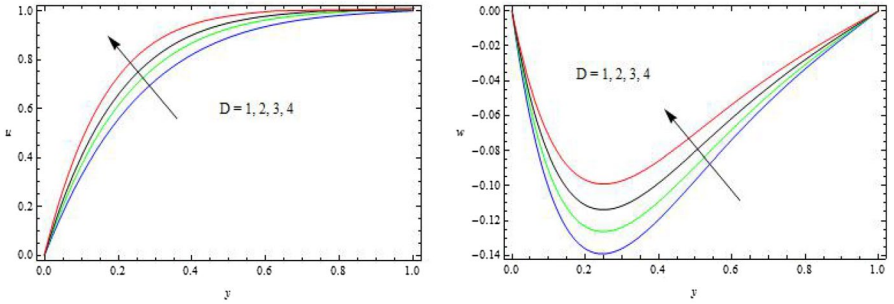

Fig. 4 The velocity profiles for u and w against D

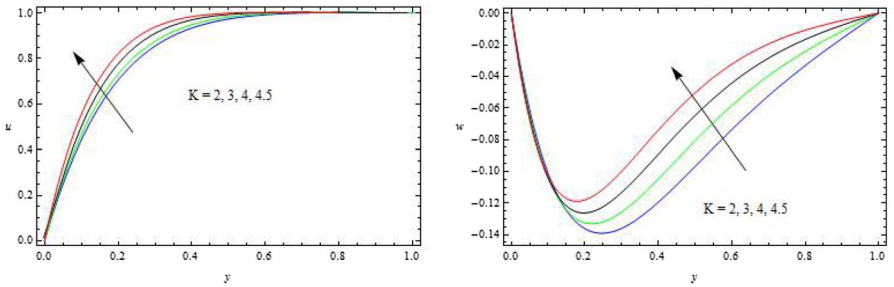

Fig. 5 The velocity profiles for u and w against K

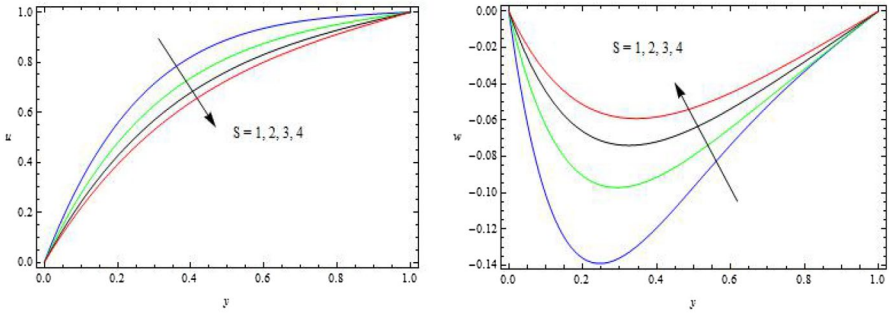

Fig. 6 The velocity profiles for u and w against S

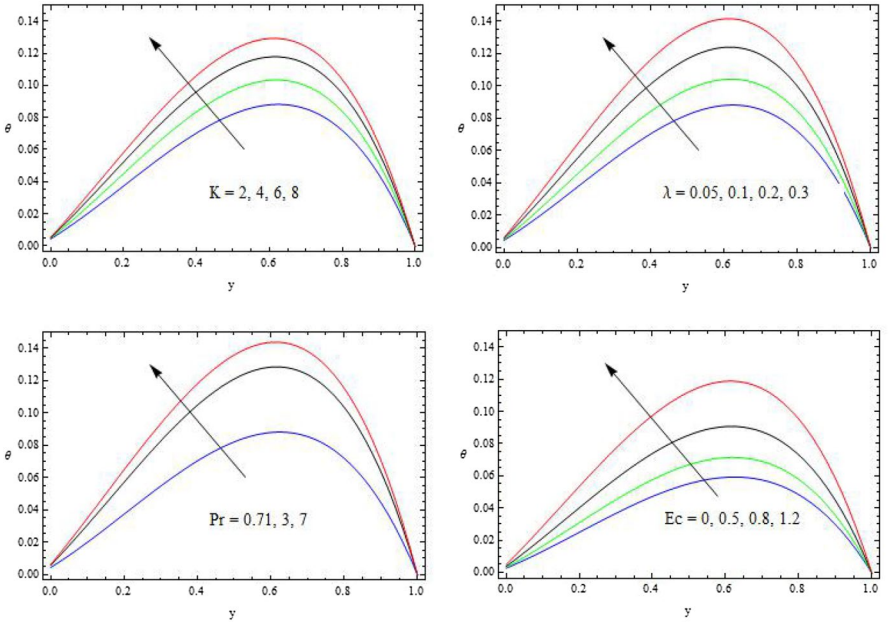

Fig. 7 The temperature profiles for θ against K, λ, Pr and Ec

$$Nu_U = -\left(\frac{\partial \theta}{\partial y}\right)_{y=1} \tag{26}$$

3 Results and discussions

The velocity profiles for u and w with time, Temperature profile for θ with time are shown in Fig. 2. It is shown the time evolution of the primary and secondary velocity profiles across the channel for a fixed set of parameter values. The primary

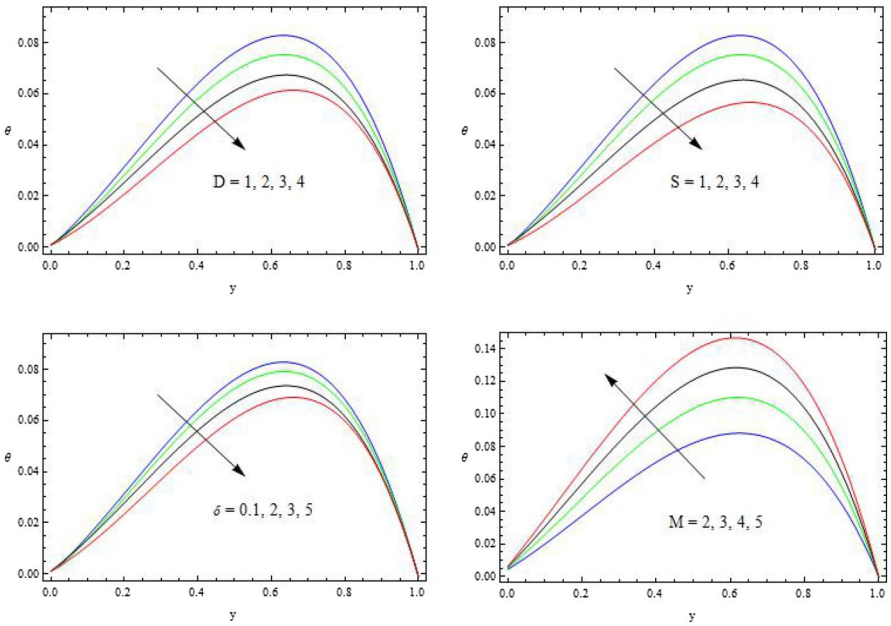

Fig. 8 The temperature profiles for θ against D, S, δ and M

velocity and secondary velocity increase from its zero value at the lower fixed plate to its maximum value at the upper moving plate. Also it exhibits the time evolution of the temperature profiles across the channel for a fixed set of parameter values. The temperature increases from its zero value at the lower fixed plate to its maximum value at the centre region of the channel.

The velocity components u and w for several values of magnetic parameter M, Darcy parameter D, rotation parameter K and second grade fluid parameter S are presented in Figs. 3, 4, 5, 6. It is seen from Fig. 3 that the primary velocity u enhances and the magnitude of the secondary velocity w retards initially and then increases with increasing values of magnetic parameter M. This is mainly due to the influence of Lorentz forces present in the magnetic field. This is an established result reported by many authors. From Fig. 4, we noticed that, the magnitudes of both the velocity components u and w are increase with increasing permeability of the porous medium. Lower the permeability lesser the fluid speed is observed in the entire fluid region.

Figure 5 shows that the primary velocity u increases and the magnitude of the secondary velocity w enhances near the stationary plate and retards near the moving plate with an increase in rotation parameter K. From the Fig. 6, the magnitude of the velocity component u reduces and w increases throughout the fluid region with increasing second grade fluid parameter S. Likewise the resultant velocity diminishes with increasing S. From the Fig. 7, an increase in λ, increases the internal heat generation within the channel due to exothermic reaction, primary to a rise in the fluid temperature.

Table 1 Shear stresses

M	D	K	S	T	τ_L		τ_U	
					τ_{x_0}	τ_{z_0}	τ_{x_1}	τ_{z_1}
2	**1**	**2**	**1**	0.5	0.153545	0.325652	0.254478	0.521045
3	1	2	1	0.5	0.198554	0.300214	0.221025	0.652102
4	1	2	1	0.5	0.245526	0.274118	0.114522	0.748905
2	**2**	2	1	0.5	0.185548	0.350026	0.298856	0.663151
2	**3**	2	1	0.5	0.198870	0.398501	0.352663	0.785549
2	1	**4**	1	0.5	0.254152	0.358874	0.221457	0.855244
2	1	**6**	1	0.5	0.285596	0.412252	0.200452	1.220033
2	1	2	**2**	0.5	0.196696	0.256099	0.214458	0.996854
2	1	2	**3**	0.5	0.201145	0.185524	0.120013	1.562236
2	1	2	1	**1.0**	0.170255	0.344528	0.288599	0.455079
2	1	2	1	**1.5**	0.192005	0.398859	0.311245	0.366525

Bold values indicate the variation of particular parameter being other parameters fixed

The fluid temperature θ increases as K. As the rotation parameter increases, the Coriolis force increases which results in an increase in temperature profiles. The fluid temperature θ increases with an increase in either Prandtl number Pr or Eckert

Table 2 Nusselt number

M	K	S	λ	Ec	δ	Pr	T	Nu_L	Nu_U
2	**2**	**1**	**0.05**	**0.5**	**0.1**	**0.71**	0.5	0.123445	0.052246
3	2	1	0.05	0.5	0.1	0.71	0.5	0.136685	0.041505
4	2	1	0.05	0.5	0.1	0.71	0.5	0.152245	0.036201
2	2	1	0.05	0.5	0.1	0.71	0.5	0.154452	0.058895
2	2	1	0.05	0.5	0.1	0.71	0.5	0.198854	0.078854
2	**4**	1	0.05	0.5	0.1	0.71	0.5	0.152248	0.085546
2	**6**	1	0.05	0.5	0.1	0.71	0.5	0.214563	0.144522
2	2	**2**	0.05	0.5	0.1	0.71	0.5	0.198854	0.083256
2	2	**3**	0.05	0.5	0.1	0.71	0.5	0.256632	0.121452
2	2	1	**0.1**	0.5	0.1	0.71	0.5	0.145228	0.035526
2	2	1	**0.2**	0.5	0.1	0.71	0.5	0.156632	0.012245
2	2	1	0.05	**0.8**	0.1	0.71	0.5	0.166895	0.099856
2	2	1	0.05	**1.2**	0.1	0.71	0.5	0.225466	0.122549
2	2	1	0.05	0.5	**2**	0.71	0.5	0.095466	0.085523
2	2	1	0.05	0.5	**3**	0.71	0.5	0.073652	0.100025
2	2	1	0.05	0.5	0.1	**3**	0.5	0.199856	0.022879
2	2	1	0.05	0.5	0.1	**7**	0.5	0.247858	0.011252
2	2	1	0.05	0.5	0.1	0.71	**1.0**	0.655256	0.012245
2	2	1	0.05	0.5	0.1	0.71	**1.5**	1.552633	0.008591

Bold values indicate the variation of particular parameter being other parameters fixed

number *Ec*. Figure 8 describes that the fluid temperature rises with an increase in either magnetic parameter *M*. A rise in the intensity of the magnetic field causes an increase in the fluid temperature within the channel. An increase in the permeability parameter *D* or second grade fluid parameter *S* or thermal conductivity variation parameter δ the temperature decreases throughout the fluid region. As δ increases, the viscous heating effect decreases and hence the fluid temperature drops.

For purposes of engineering design, the shear stresses at the channel plates are important. We can then obtain the shear stresses at the plates due to the primary and the secondary flows on separating into real and imaginary parts of the complex Eqs. (18) and (19). Numerical results of the non-dimensional shear stresses τ_{x_0} and τ_{z_0} at the lower plate $y = 0$ due to the primary and the secondary flows and the shear stresses τ_{x_1} and τ_{z_1} at the upper plate $y = 1$ due to the primary and the secondary flows are presented in Table 1 for several values of magnetic parameter *M*, rotation parameter *K*, Darcy parameter D and second grade fluid parameter *S*. The flow separation does not occur as shear stresses are never zero. The positive values of the shear stress τ_{x_1} at the moving plate $y = 1$ due to the secondary flow actually confirm the existence of a backflow for the secondary velocity. At the lower plate, the shear stress τ_{x_0} increases whereas the magnitude of the shear stress τ_{z_0} decreases as *M* increases. The reversal behaviour is observed for the upper plate with *M*. As the magnetic field intensity increases, the velocity gradient increases at the lower fixed plate and decreases at the upper moving plate due to the resistance effect of Lorenz force at the upper plate. The similar behaviour is observed with increasing second grade fluid parameter *S*. Both the stress components enhances with increasing rotation parameter *K* at the lower plate whereas τ_{x_1} reduces and τ_{z_1} increases with increasing *K* on upper plate. This is because the rotational drag force leads to an increase in the fluid velocity gradient at both plate surfaces. At both the plates, the stresses enhance with increasing Darcy parameter *D*. As expected, a progress in time the velocity components are boosted up, leading to an increase in the shear stresses at the lower plate. On other hand, the shear stress τ_{x_1} increases whereas the shear stress τ_{z_1} decreases as time increases.

Table 3 Comparison of results for primary velocity component *u* $\delta = 0.1,\ Ec = 0.5,\ t = 0.5,\ \lambda = 0.05,\ \mathrm{Pr} = 0.71,\ y = 0.2$

M	*K*	S	Previous results Das et al. [8] $u\ D \to 0$	Present results *u*
2	**2**	**1**	0.255665	0.255659
3			0.201478	0.201466
4			0.185547	0.185536
	4		0.298857	0.298848
	6		0.354478	0.354469
		2	0.336698	0.336688
		3	0.378857	0.378844

Bold values indicate the variation of particular parameter being other parameters fixed

We noticed that from the Table 2 Nu_L increases with an increase in M or time t and Nu_U reduces as M increases. It is clear that the rate of heat transfer is less near the moving plate in the presence of magnetic field. The rate of heat transfer Nu_L or Nu_U increase with Ec or D or K. Nu_L increases whereas the rate of heat transfer Nu_U reduces when Prandtl number Pr increases. This may be also explained by the fact that frictional forces become dominant at the stationary plate for increasing values of Prandtl number Pr and hence yield greater heat transfer rate. Hence, Prandtl number can be used to control the rate of cooling in flow systems. Similar behaviour is observed for λ. The rate of heat transfer Nu_L decreases whereas the rate of heat transfer Nu_U increases with an increase in δ. As δ increases, the thermal conductivity of fluid enhances and hence heat can diffuse from the moving plate faster. As a result, the rate of heat transfer at the moving plate increases. The identical behavior is monitored for the second grade fluid parameter S. Table 3 represent comparison of results for primary velocity component u. We observed that, good agreement with the previous results of Das et al. [8] when $D \to 0$.

4 Conclusions

In this paper, a transient hydromagnetic Couette flow through porous medium and heat transfer of a reactive viscous incompressible electrically conducting fluid between two infinitely long horizontal parallel plates in the presence of a uniform transverse magnetic field in a rotating system when one of the plate is set into uniform accelerated motion under Arrhenius reaction rate has been presented. The conclusions are made as the following.

1. The magnitude of the velocity has been significantly modified due to combined effects of magnetic field, permeability and rotation.
2. The velocity within the channel is accelerated when time progresses.
3. The temperature within the channel reduces due to increasing variable thermal conductivity while it enhances for increasing values of magnetic parameter or Frank-Kamenetskii parameter or rotation or Eckert number.
4. The rotation enhances the absolute value of the shear stresses at the lower plate.
5. The shear stress due to the primary flow enhances whereas the shear stress due to the secondary flow reduces at the lower plate for increasing M.
6. Nusselt number at the lower plate enhances whereas at the upper plate reduces as magnetic parameter or Prandtl number or time increases.

Funding The authors have not getting any funding from funding agencies.

Compliance with ethical standards

Research involving human participants and/or animals My research is only mathematical modelling. No human participants or animals involving in this research.

Conflict of interest The authors have not conflict of interest in this manuscript.

Ethical approval The authors have got moral support from Dept of Mathematics, Rayalaseema University, Kurnool for doing this manuscript.

Informed consent The authors have not taken any permission.

References

1. AnwarBég, O., S. Lik, J. Zueco, and R. Bhargava. 2010. Numerical study of magnetohydrodynamic viscous plasma flow in rotating porous media with Hall currents and inclined magnetic field influence. *Communications Nonlinear Science and Numerical Simulation* 15: 345–359.
2. Chandran, P., N.C. Sacheti, and A.K. Singh. 1993. Effect of rotation on unsteady hydromagnetic Couette flow. *Astrophysics Space Science* 202: 110.
3. Chauhan, D.S., and R. Agrawal. 2012. Effects of Hall current on MHD Couette flow in a channel partially filled with a porous medium in a rotating system. *Meccanica* 47: 405–421.
4. Chinyoka, T., and O.D. Makinde. 2011. Analysis of transient generalized Couette flow of a reactive variable viscosity third-grade liquid with asymmetric convective cooling. *Mathematical Computer Modeling* 54: 160–174.
5. Cramer, K.R., and S.I. Pai. 1973. *Magnetofluid dynamics for engineers and applied physicists*. New York: McGraw-Hill.
6. Das, S., S.L. Maji, M. Guria, and R.N. Jana. 2009. Unsteady MHD Couette flow in a rotating system. *Mathematical Computer Modeling* 50: 1211–1217.
7. Das, S., B.C. Sarkar, and R.N. Jana. 2011. Hall effects on MHD Couette flow in rotating system. *International Journal of Computer Applications* 35 (13): 22–30.
8. Das, S., R.N. Jana, and O.D. Makinde. 2016. Transient hydromagnetic reactive Couette flow and heat transfer in a rotating frame of reference. *Alexandria Engineering Journal* 55: 635–644.
9. Gosh, S.K., Anwar O. Beg, and M. Narahari. 2009. Hall effects on MHD flow in a rotating system with heat transfer characteristics. *Meccanica* 44: 741–765.
10. Gosh, S.K., Anwar O. Beg, and M. Narahari. 2013. A study of unsteady rotating hydromagnetic free and forced convection in a channel subject to forced oscillation under an oblique magnetic field. *Journal Applied Fluid Mechanics* 6 (2): 213–227.
11. Jana, R.N., N. Datta, and B.S. Mazumder. 1977. Magnetohydrodynamic Couette flow and heat transfer in a rotating system. *Journal of Physics Society Japan* 42: 1034–1039.
12. Jana, R.N., and N. Datta. 1980. Hall effects on MHD Couette flow in a rotating system. *Czechoslovak Journal of Physics* 330: 659.
13. Jha, B.K., and C.A. Apere. 2010. Combined effect of hall and ion slip currents on unsteady MHD couette flows in a rotating system. *Journal of Physics Society Japan* 79: 104401. **(9 pages)**.
14. Jha, B.K., and C.A. Apere. 2011. Time-dependent MHD Couette flow in a rotating system with suction/injection. *Z Angew Mathematics and Mechanics* 91 (10): 832–842.
15. Jha, B.K., and C.A. Apere. 2012. Time-dependent MHD Couette flow of rotating fluid with Hall and ion-slip currents. *Applied Mathematics and Mechanics* 33: 399–410.
16. Jha, B.K., B.Y. Isah, and I.J. Uwanta. 2015. Unsteady MHD free convective Couette flow between vertical porous plates with thermal radiation. Journal of King Saud University –. *Science* 27: 338–348.
17. Jha, B.K., B. Aina, and S. Isa. 2015. Fully developed MHD natural convection flow in a vertical annular microchannel: an exact solution. *Journal of King Saud University Science* 27: 253–259.
18. Kobo, N.S., and O.D. Makinde. 2014. Second law analysis for a variable viscosity reactive Couette flow under Arrhenius kinetics. *Mathematical Problems in Engineering* 1–15: 278104.
19. Makinde, O.D. 2007. On steady flow of a reactive variable viscosity fluid in a cylindrical pipe with an isothermal wall. *International Journal of Numerical Methods in Heat and Fluid Flow* 17 (2): 187–194.

20. Makinde, O.D., and O.O. Onyejekwe. 2011. A numerical study of MHD generalized Couette flow and heat transfer with variable viscosity and electrical conductivity. *Journal of Magnetism and Magnetic Meterials* 323: 2757–2763.
21. Makinde, O.D. 2014. Thermal analysis of a reactive generalized Couette flow of power law fluids between concentric cylindrical pipes. *European Physics Journal Plus* 129: 2–9.
22. Makinde, O.D., and O. Franks. 2014. On MHD unsteady reactive Couette flow with heat transfer and variable properties. *Central European Journal of Engineering* 4: 54–63.
23. Muzychka, Y.S., and M.M. Yovanovich. 2006. Unsteady viscous flows and Stokes' first problem. *Proceedings of IMECE* 14301: 1–11.
24. Nanda, R.S., and H.K. Mohanty. 1970. Hydromagnetic flow in a rotating channel. *Applied Science Residues* 24: 65–78.
25. Nayak, A., and G.C. Dash. 2015. Magnetohydrodynamic couple stress fluid flow through a porous medium in a rotating channel. *Journal Engineering Thermophysics* 24 (3): 283–295.
26. Ramzan, M., and M. Bilal. 2015. Time dependent MHD nano-second grade fluid flow induced by permeable vertical sheet with mixed convection and thermal radiation. *PLoS One* 10 (5): e0124929. https://doi.org/10.1371/journal.pone.0124929.
27. Ramzan, M., M. Bilal, U. Farooq, and Jae DongChung. 2016. Mixed convective radiative flow of second grade nanofluid with convective boundary conditions: An optimal solution. *Results in Physics* 6: 796–804. https://doi.org/10.1016/j.rinp.2016.10.011.
28. Ramzan, M., M. Bilal, Jae Dong Chung, and U. Farooq. 2016. Mixed convective flow of Maxwell nanofluid past a porous vertical stretched surface—an optimal solution. *Results in Physics* 6: 1072–1079. https://doi.org/10.1016/j.rinp.2016.11.036.
29. Ramzan, M., F. Yousaf, M. Farooq, and J.D. Chung. 2016. Mixed convective visco-elastic nanofluid flow past a porous media with Soret–Dufour effects. *Communications in Theoretical Physics* 66 (1): 133. https://doi.org/10.1088/0253-6102/66/1/133.
30. Ramzan, M., M. Bilal, Jae Dong Chung, Lu Dian Chen, and Umer Farooq. 2017. A mathematical model has been established to study the magnetohydrodynamic second grade nanofluid flow past a bidirectional stretched surface. *Physics of Fluids* 29: 093102. https://doi.org/10.1063/1.4986822.
31. Ramzan, M., M. Bilal, and Jae Dong Chung. 2017. Numerical simulation of magnetohydrodynamic radiative flow of Casson nanofluid with chemical reaction past a porous media. *Journal of Computational and Theoretical Nanoscience* 14 (12): 5788–5796. https://doi.org/10.1166/jctn.2017.7013.
32. Ramzan, M., J.D. Chung, and N. Ullah. 2017. Partial slip effect in the flow of MHD micropolar nanofluid flow due to a rotating disk—a numerical approach. *Results in Physics* 7: 3557–3566. https://doi.org/10.1016/j.rinp.2017.09.002.
33. Seth, G.S., R.N. Jana, and M.K. Maity. 1982. Unsteady hydromagnetic Couette flow in a rotating system. *International Journal of Engineering Science* 20: 989–999.
34. Seth, G.S., and M.K. Maiti. 1982. MHD Couette flow and heat transfer in a rotating system. *Indian Journal of Pure and Applied Physics* 13: 931–945.
35. Seth, G.S., and S.K. Ghosh. 1986. Effect of Hall current on unsteady hydromagnetic flow in a rotating channel with oscillating pressure gradient. *Indian Journal of Pure and Applied Physics* 17 (6): 819–826.
36. Seth, G.S., MdS Ansari, and R. Nandkeolyar. 2010. Unsteady hydromagnetic Couette flow induced due to accelerated movement of one of the porous plates of the channel in a rotating system. *International Journal of Applied Mathematics and Mechanics* 6 (7): 24–42.
37. Singh, K.D., and R. Pathak. 2012. Effect of rotation and Hall current on mixed convection MHD flow through a porous medium filled in a vertical channel in presence of thermal radiation. *Indian Journal of Pure and Applied Physics* 50: 77–85.
38. Seth, G.S., and J.K. Singh. 2013. Effects of Hall current on unsteady MHD Couette flow of class-II in a rotating system. *Journal of Applied Fluid Mechanics* 6 (4): 473–484.
39. Seth, G.S., B. Kumbhakar, and R. Sharma. 2015. Unsteady hydromagnetic natural convection flow of a heat absorbing fluid within a rotating vertical channel in porous medium with Hall effects. *Journal of Applied Fluid Mechanics* 8 (4): 767–779.
40. Seth, G.S., and J.K. Singh. 2015. Mixed convection hydromagnetic flow in a rotating channel with Hall and wall conductance effects. *Applied Mathematical Modeling* 40 (4): 2783–2803. https://doi.org/10.1016/j.apm.2015.10.015.
41. Singh, A.K., P. Chandran, and N.C. Sacheti. 1994. Transient effects on magnetohydrodynamic Couette flow with rotation: accelerated motion. *International Journal of Engineering Science* 32: 133–139.

42. Swarnalathamma, B.V., and M. Veera Krishna. 2016. Peristaltic hemodynamic flow of couple stress fluid through a porous medium under the influence of magnetic field with slip effect. *AIP Conference Proceedings* 1728: 020603. https://doi.org/10.1063/1.4946654.
43. Theuri, D., and O.D. Makinde. 2014. Thermodynamic analysis of variable viscosity MHD unsteady generalized Couette flow with permeable walls. *Applied and Computational Mathematics* 3 (1): 1–8.
44. VeeraKrishna, M., and M. Gangadhar Reddy. 2016. MHD free convective rotating flow of Visco-elastic fluid past an infinite vertical oscillating porous plate with chemical reaction. *IOP Conference Series: Materials Science and Engineering* 149: 012217. https://doi.org/10.1088/1757-899X/149/1/012217.
45. VeeraKrishna, M., and G. Subba Reddy. 2016. Unsteady MHD convective flow of Second grade fluid through a porous medium in a Rotating parallel plate channel with temperature dependent source. *IOP Conference Series: Materials Science and Engineering* 149: 012216. https://doi.org/10.1088/1757-899X/149/1/012216.
46. VeeraKrishna, M., and B.V. Swarnalathamma. 2016. Convective heat and mass transfer on MHD peristaltic flow of williamson fluid with the effect of inclined magnetic field". *AIP Conference Proceedings* 1728: 020461. https://doi.org/10.1063/1.4946512.
47. Veera Krishna, M., B.V. Swarnalathamma, and J. Prakash. 2018. "Heat and mass transfer on unsteady MHD Oscillatory flow of blood through porous arteriole. *Applications of Fluid Dynamics, Lecture Notes in Mechanical Engineering, XXII*. https://doi.org/10.1007/978-981-10-5329-0_14.
48. Veera Krishna, M., G. Subba Reddy, and A.J. Chamkha. 2018. Hall effects on unsteady MHD oscillatory free convective flow of second grade fluid through porous medium between two vertical plates. *Physics of Fluids* 30: 023106. https://doi.org/10.1063/1.5010863.
49. Veera Krishna, M., and A.J. Chamkha. 2018. Hall effects on unsteady MHD flow of second grade fluid through porous medium with ramped wall temperature and ramped surface concentration. *Physics of Fluids* 30: 053101. https://doi.org/10.1063/1.5025542.